# Biomimetic Peptide-Enriched Electrospun Polymers: A Photoelectron and Infrared Spectroscopy Study

**G. Iucci,[1] F. Ghezzo,[2] R. Danesin,[2] M. Modesti,[2] M. Dettin[2]**

[1]*Department of Physics, INSTM and CISDiC, University "Roma Tre," Via della Vasca Navale, 84 00146 Rome, Italy*
[2]*Department of Chemical Process Engineering, University of Padova, Via Marzolo, 9-35131 Padova, Italy*

Received 28 April 2011; accepted 28 April 2011
DOI 10.1002/app.34768
Published online 10 August 2011 in Wiley Online Library (wileyonlinelibrary.com).

**ABSTRACT:** Biomimetic polymer nanofibers of poly(ε-caprolactone) and poly(L-lactide–caprolactone) copolymer were prepared by electrospinning. Modifications of the polymer nanofibers aimed at improving their biomimetic properties were performed by two different routes: (1) immobilization of an adhesion peptide, which mimicked the adhesion sequence of the extracellular matrix protein fibronectin, on the polymer surface and (2) incorporation of self-complementary oligopeptides, which showed alternated hydrophilic and hydrophobic side chain groups and was capable of generating extended ordered structures by self-assembling, into the polymer nanofibers. The structure of the polymer/peptide nanofibers was investigated by X-ray photoelectron and Fourier transform infrared spectroscopies. © 2011 Wiley Periodicals, Inc. J Appl Polym Sci 122: 3574–3582, 2011

**Key words:** polyesters; peptides; X-ray

## INTRODUCTION

Biomaterial scaffolds have attracted increasing interest for the preparation of biomedical devices for tissue engineering; to promote cell colonization and, therefore, cell growth, scaffolds must mimic the extracellular matrix (ECM) in the best possible way. Electrospinning is one of the most promising techniques for the preparation of biomaterial scaffolds and for skin and cartilage reconstruction, artificial nerves, and especially, blood vessels.[1–3]

In the electrospinning technique, polymeric nanofibers are obtained by the ejection of a polymeric solution from a syringe through a needle to a collector surface; a high voltage is applied between the needle and the collector. Compared to other extrusion techniques, electrospinning has the advantage of producing fibers having a very small caliber, in the 5–500-μm range.

During the past few years, electrospun nanofibers of biocompatible polymers, such as poly(ε-caprolactone) (PCL) and copolymers, have been studied as promising candidates for small-caliber blood vessels. The biomimetic properties of the polymer nanofibers can be improved by surface modifications[2] or by protein incorporation in the polymer blend.[4]

ECM proteins play a major role in the adhesion of several cell types to the material surface; cell adhesion can be promoted by the immobilization of oligopeptides, which mimics the adhesion sequence of ECM proteins. Fibronectin is one of the main ECM proteins responsible for cell adhesion, which takes place via interaction between the RGD binding sequence of fibronectin and cell membrane integrin receptors. Immobilization of an entire protein on a surface can result in protein denaturation and a loss in the bioactivity, a drawback that can be prevented by the anchoring of short biomimetic peptides; this reproduces the protein receptor binding site, such as the $(GRGDSP)_4K$ peptide mimicking the RGD bending site of fibronectin.[5,6]

Self-assembling (SA) peptides are another class of materials studied for scaffold preparation; self-complementary amphiphilic oligopeptides, which show alternating positively and negatively charged side chains separated by hydrophobic side chains, can generate extended ordered structures by SA from aqueous solutions.[7,8] The most widely studied SA peptide is EAK, the so-called molecular lego, a 16-unit oligopeptide consisting of a periodic sequence of the amino acids L-alanine, L-glutamic acid, and L-lysine.[9,10] Interaction between peptide molecules in β-sheet conformation takes place via hydrogen bonds between the peptide groups of the backbone within the sheets and by hydrophobic or ionic interaction of the side chains between the different sheets. The structure of SA EAK in the plane perpendicular to the β sheets is shown in Figure 1.

We extended our investigation to related SA peptides, having amino acidic residues with different side chain structures; the amino acid sequence of the investigated peptides is shown in Table I. In the newly

*Correspondence to:* G. Iucci (iucci@uniroma3.it).
Contract grant sponsor: Ministero dell'Istruzione, dell'Universtità e della Ricerca (MIUR).

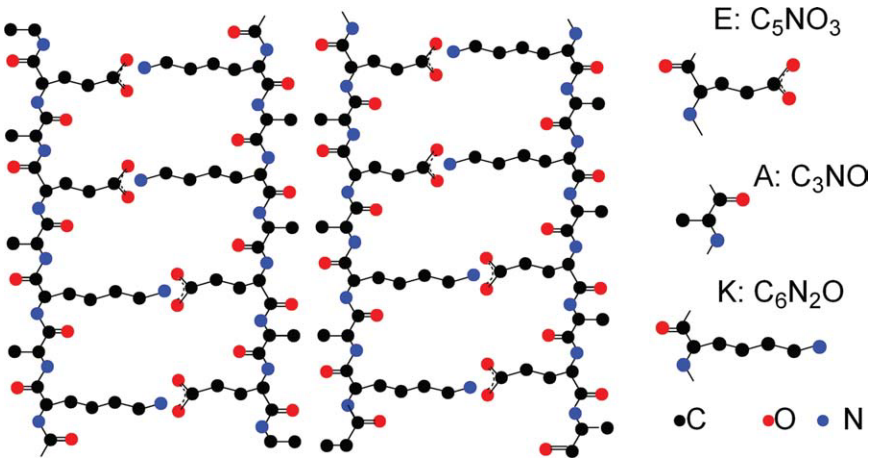


**Figure 1** Structure of SA EAK. [Color figure can be viewed in the online issue, which is available at wileyonlinelibrary.com.]

synthesized 16-unit oligopeptides, we modified the side chains with respect to EAK by replacing L-glutamic with L-aspartic acid (DAK) and L-alanine with L-α-aminobutyric acid (Abu; EAbuK) or with L-tyrosine (EYK). Finally, new peptides were synthesized containing the RGD motif coupled to EAK (RGD–EAK) or to a scrambled EAK sequence (RGD–EAKsc).[11,12]

In this article, we present a photoelectron spectroscopy study on biomimetic polymeric scaffolds consisting of nanofibers of PCL and poly(L-lactide–caprolactone) copolymer [P(LLA–CL)] prepared by electrospinning before and after the immobilization of a peptide containing the RGD (Arg–Gly–Asp) adhesion motif on the polymer surface. The investigated peptide, whose structure is shown in Table I and in Figure 2, contained two photoreactive azido groups at the C— and N— terminals.

The immobilization of the RGD peptide on the polymer nanofibers was carried out by incubation of the polymeric electrospun scaffold in peptide solutions at different concentrations and subsequent UV irradiation; peptide immobilization on the polymer surface took place via reaction of the two terminal azido groups, as shown in Figure 2(B). The immobilized RGD sequence was expected to increase the polymer bioactivity, whereas the crosslinking between the nanofibers [see Fig. 2(C)] might have improved their mechanical properties.

A further technique aimed at improving nanofiber bioactivity consisted of peptide incorporation into the polymer blend; therefore, we prepared polymer nanofibers by electrospinning a mixed PCL/SA peptide solution for all of the SA peptides shown in Table I. The surface of the nanofibers obtained was investigated by X-ray photoelectron spectroscopy (XPS) and Fourier transform infrared (FTIR) spectroscopy with the aim of revealing the structure of the peptide incorporated into the PCL nanofibers.

XPS, yielding information on the outmost 50–100 Å of the surface, has been widely used to investigate polymer nanofibers prepared by electrospinning[13–19] and to study the immobilization of proteins or other biomolecules onto the nanofibers.[14–19] FTIR spectroscopy has also been widely employed in the characterization of polymer nanofibers,[20–23] particularly of nanofibers containing immobilized biomolecules;[17–19,21–23] the possibility of investigating the peptide bond vibrations yields information on the immobilized protein structure.[23–25]

## EXPERIMENTAL

### Peptide synthesis

The RGD peptide was synthesized as a *p*-amino analogue with Fmoc chemistry with a Syro-I synthesizer

**TABLE I**
**Chemical Structure of the Investigated Peptides**

| Peptide sequence | Name |
|---|---|
| H—Phe(*p*-$N_3$)—(Gly—Arg—Gly—Asp—Ser—Pro)$_4$—Phe(*p*-$N_3$)—$NH_2$ | RGD |
| H—(Ala—Glu—Ala—Glu—Ala—Lys—Ala—Lys)$_2$—$NH_2$ | EAK |
| H—(Ala–Asp—Ala—Asp—Ala—Lys—Ala—Lys)$_2$—$NH_2$ | DAK |
| H—(Abu—Glu—Abu—Glu—Abu—Lys—Abu—Lys)$_2$—$NH_2$ | EAbuK |
| H—(Tyr—Glu—Tyr—Glu—Tyr—Lys—Tyr—Lys)$_2$—$NH_2$ | EYK |
| H—Arg—Gly—Asp—(Ala—Glu—Ala—Glu—Ala—Lys—Ala—Lys)$_2$—$NH_2$ | RGD–EAK |
| H—Arg—Gly—Asp—Ala—Ala—Lys—Ala—Glu—Ala—Glu—Ala—Ala—Glu—Lys—Ala—Lys—Ala—Glu—Lys—$NH_2$ | RGD–EAKsc |

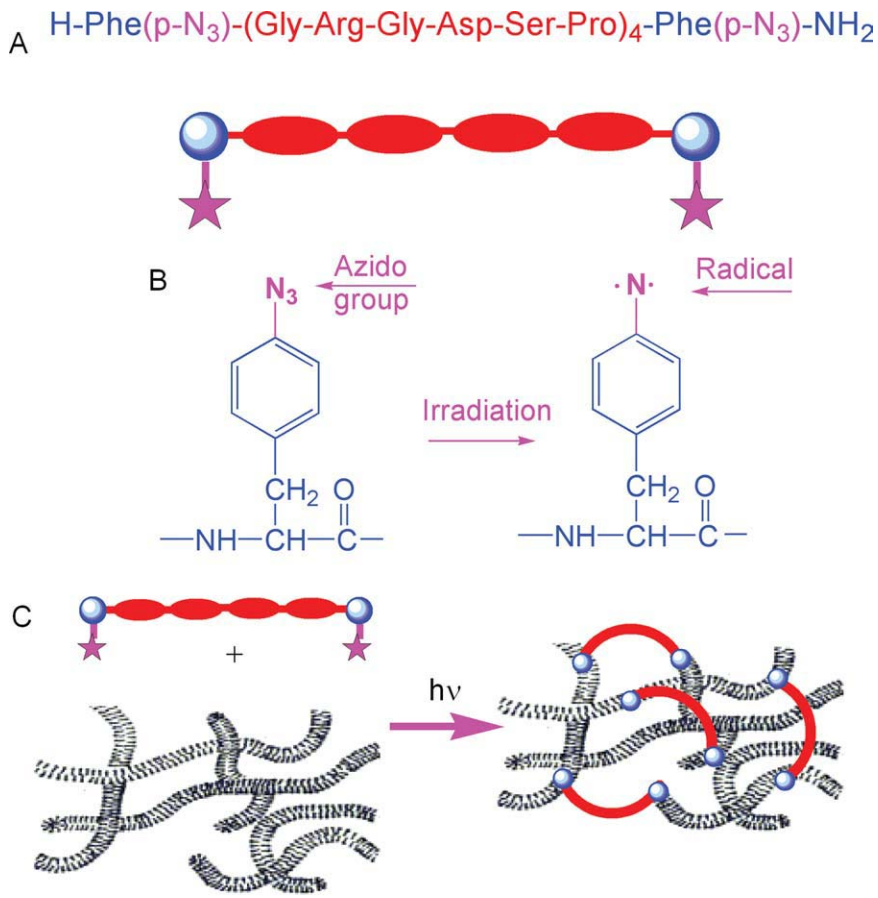


**Figure 2** (A) Sequence and structure of the RGD peptide, (B) photoreaction of the azido group, and (C) crosslinking of the polymer nanofibers. [Color figure can be viewed in the online issue, which is available at wileyonlinelibrary.com.]

(Multisyntech Gmbh, Witten, Germany). After the conversion of amino groups into azido groups by reaction in solution with sodium nitrite and sodium azide, the crude product was purified by reverse-phase chromatography (RP-HPLC) and characterized by mass spectrometry.

SA peptides were synthesized as C-terminal amides by solid-phase methods with a fully automated peptide synthesizer (Applied Biosystems model 431A; Foster City, CA) via Fmoc chemistry and purified by RP-HPLC.[26] Peptide identity and homogeneity were evaluated with analytical RP-HPLC, capillary electrophoresis, and mass spectrometric analysis (electrospray ionisation- time of flight (ESI-TOF)). The homogeneity of each peptide was over 98%.

### Electrospinning and peptide immobilization

Films of P(LLA–CL) (70 : 30; PURAC Biochem-Gorinchen, Holland) or PCL (number-average molecular weight = 60,000, Da Sigma Aldrich, St. Louis, MO) nanofibers were prepared by an electrospinning process that was carried out under the following conditions: solution = 10 wt % in a dichloromethane (DCM):dimethylformamide = 70 : 30 w/w solution; 0.4-mm diameter needle; supply at 1 mL/h; tension = 8kV.[27] The aluminum foil (15 × 15 $cm^2$) used as the collector was cut in circular samples of 1.2 diameter.

Immobilization of the RGD peptide, whose chemical structure is shown in Figure 2 and Table I on the nanofibers surface was obtained through the incubation of samples with a solution of 1 mg of peptide in 1 mL of MilliQ water (or 0.1 mg/mL or 0.01 mg/mL) for 1 h at room temperature. The samples were dried *in vacuo* in the presence of $P_2O_5$. Each sample was irradiated for 1 h at 254 and 366 nm (distance from the lamp = 1 cm).

PCL nanofibers containing SA peptides incorporated into the polymer solution were prepared by dissolution of only PCL or SA peptides plus PCL (at a 5 : 95 w/w ratio) in 1,1,1,3,3,3-hexafluorine-2-propanol at a 10% w/w concentration.

In the electrospinning process, the solution was released from a 5-mL syringe through a 27-G needle at a 1 mL/h flux speed by a volumetric pump; the voltage between the collector and solution was 16 kV. Fibers were collected on a circular aluminum foil collector (1.2 cm diameter) located at a 15-cm

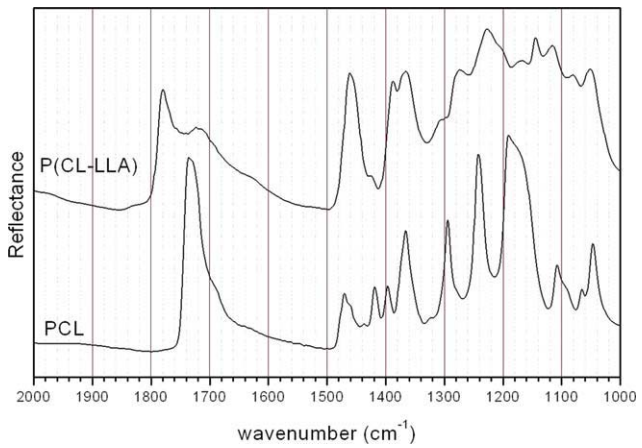


**Figure 3** FTIR spectra of PCL and P(LLA–CL) in the 2000–1000-$cm^{-1}$ range. [Color figure can be viewed in the online issue, which is available at wileyonlinelibrary.com.]

distance from the needle. After deposition, samples were dried *in vacuo* in the presence of $P_2O_5$.

Aging was performed on selected samples by incubation of the polymer nanofibers with saline phosphate buffer in MilliQ water (150 m*M* NaCl, 10 m*M* sodium phosphate, pH 7.4) for 3 days and subsequent washing with MilliQ water and drying *in vacuo*.

### XPS

XPS investigations were performed in an instrument of our own construction and design equipped with a 150-mm mean radius hemispherical electron analyzer and a 16-channel detector. Mg Kα nonmonochromatized X-ray radiation ($h\nu$ = 1253.6 eV) was used to record peptide (C1s, N1s, O1s) and polymer (C1s, O1s) core-level spectra on the respective samples. In all of the investigated samples, the Al2p signal form the Al foil substrate was too low to be detected; this indicated the presence of a thick mat of polymer nanofibers. The spectra were energy referenced to the C1 signal of aliphatic carbons located at a binding energy (BE) of 285.0 eV.[28] The standard deviation on the measured BE values was ±0.1 eV. Atomic ratios were calculated from the peak intensities with Scofield's cross sections and experimentally determined sensitivity factors. A curve-fitting analysis of the C1s, N1s, and O1s spectra was performed with Gaussian curves as fitting functions.

### FTIR spectroscopy

Reflection absorption infrared spectroscopy (RAIRS) of the polymer nanofibers deposited onto Al foil were recorded in the range 4000–400 $cm^{-1}$ by means of a Vector 22 (Bruker Optics, Ettlingen, Germany) FTIR interferometer equipped with a deuterated triglycine sulphate (DTGS) detector and with a reflectance/grazing angle accessory (Specac); the incidence angle of the impinging radiation was 70°. A curve-fitting analysis of the FTIR spectra was performed with Gaussian curves as fitting functions.

## RESULTS AND DISCUSSION

### Polymeric nanofiber characterization

Before studying peptide immobilization on the polymer nanofibers, we investigated the chemical structure of the nanofiber mats by RAIRS and XPS.

The measured FTIR spectra of PCL and P(LLA–CL) are shown in Figure 3; the peak position and assignment are summarized in Table II. Table II also reports a comparison with literature data for PCL[29,30] and PLLA and poly(L-lactide)[31] polymers. The most prominent peaks in the spectra of both PCL and PLLA were related to the ester groups, namely, C=O and C—O—C stretching modes (see Table II). The spectrum of the PCL nanofibers was in excellent agreement with the literature data. The spectrum of the P(LLA–CL) resulted from the combination of the spectra of PCL and PLLA; particularly, in the C=O stretching region, the two

**TABLE II**
**FTIR Spectra of PCL and P(LLA–CL) and Comparison with Literature Data[29–31]**

| Assignment | PCL literature value 1 | PCL literature value 2 | PCL measured | PLA literature value | P(LLA–CL) measured value |
|---|---|---|---|---|---|
| C=O stretching | | | | 1750 | 1779 s |
| | 1721 | 1730 | 1730 s | | 1715 m |
| C—H bending | 1471 | | 1470 w | 1460 | 1460 s |
| | 1418 | | 1419 w | | 1420 sh |
| | 1397 | | 1396 w | 1380 | 1395 m |
| $CH_2$ wagging and twisting | 1366 | | 1366 m | 1360 | 1365 s |
| | 1294 | | 1294 m | 1280 | 1280 sh |
| C—O stretching | 1240 | 1242 | 1242 s | 1200 | 1226 s |
| C—O—C asymmetric stretching | 1166 | 1190 | 1188 s | 1140 | 1144 m |
| | 1108 | | 1106 w | 1080 | 1080 w |
| C—O—C symmetric stretching | 1065 | | 1065 sh | 1043 | |
| | 1045 | | 1047 m | | 1052 w |

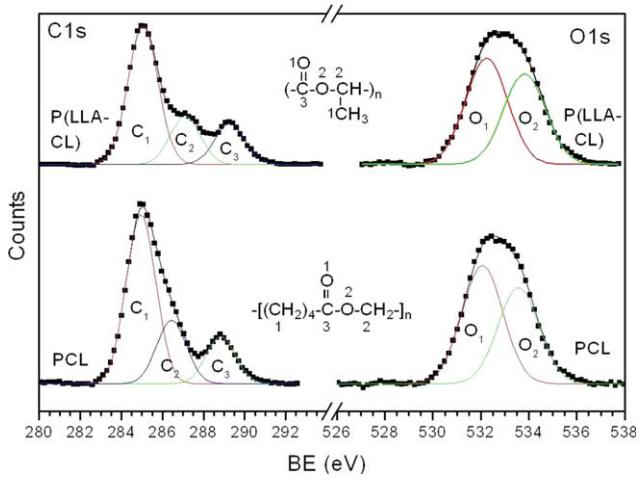


**Figure 4** C1s and O1s spectra of PCL and P(LLA–CL) and related curve-fitting analysis. Markers represent experimental points, and lines represent fitting components and calculated spectra. The chemical structures of PCL and PLLA are also shown. [Color figure can be viewed in the online issue, which is available at wileyonlinelibrary.com.]

contributions from the parent polymers could be clearly distinguished.

The C1s and O1s spectra recorded for pristine PCL and P(LLA–CL) electrospun mats and the related curve-fitting analyses are shown in Figure 4. The chemical structures of PCL and PLLA are also shown in the figure; carbon and oxygen atoms having similar chemical environments in the two polymers are labeled with the same number. According to Beamson and Briggs,[32] the C1s spectra of PCL and PLLA consist of three signals, one related to aliphatic carbons and labeled 1 ($C_1$) in the polymer structures shown in Figure 2, one related to C—O carbons ($C_2$), and one related to O—C=O carbons ($C_3$), in increasing BE order. The BEs measured from the curve-fitting analysis for the two polymer films, shown in Table III, were in good agreement with the literature data[32] for the respective polymers [PLLA was used for comparison for the P(LLA–CL) film]. The BE value of $C_2$ was slightly higher for P(LLA–CL) than for PCL because $C_2$ in PLLA was also α to a carbonyl group.

On the basis of the polymer chemical structure, the expected numeric ratios between the three different types of carbon atoms were $C_1/C_2/C_3 = 4/1/1$ for PCL, 1/1/1 for PLLA, and therefore, 1.9/1/1 for P(LLA–CL) (70–30). The O1s spectra of PCL and PLLA showed two peaks related to C=O ($O_1$) and C—O ($O_2$) oxygens, respectively; the expected atomic ratio was $O_1/O_2 = 1/1$ for both polymers. Table III also shows the measured atomic ratios for the two polymer films and the related calculated values; the agreement between the measured and calculated data was quite good. The $C_1/C_3$ and C/O atomic ratios were higher than the expected yield; this could have been due to a slight excess of aliphatic carbons ($C_1$), particularly for P(LLA–CL), because of low carbon contamination that can never be completely avoided in XPS measurements.

## RGD immobilization

The immobilization of the RGD peptide on the polymer surface took place for both materials, as evidenced by the presence of an N1s peak at a BE of 400.0 eV; this was in agreement with the expected value for the peptide amide nitrogens.[28] The N1s spectra recorded for the samples prepared at the higher peptide concentration for both polymeric substrates are shown in Figure 5. The N1s signal could be detected even for the lowest peptide concentration (0.01 mg/mL). The amount of immobilized peptide, measured by the N/C and N/O ratios, increased with peptide concentration of the mother solution, as shown in Table IV. A plot of the measured N/C and N/O ratios as a function of peptide concentration is shown in Figure 6; the trend was very similar for the two polymer mats. The calculated atomic ratio for the RGD peptide on the basis of the amino acid composition were N/C = 0.36 and N/O = 1.11 (also shown in Table IV). The reported data yielded evidence of successful immobilization of the RGD adhesion peptide onto the surface of

**TABLE III**
**Measured (meas) Binding Energies for C1s and O1s Signals of PCL and P(LLA–CL) and Comparison with Literature Data (ref) for PCL and PLLA[32] and the Calculated (calc) and Measured (meas) Atomic Ratios for PCL, PLLA, and P(LLA–CL)**

| | BE (eV) | | | | | Atomic ratios | | | |
|---|---|---|---|---|---|---|---|---|---|
| Polymer | $C_1$ (C—C) | $C_2$ (C—O) | $C_3$ (O—C=O) | $O_1$ (O=C) | $O_2$ (O—C) | $C_1/C_3$ | $C_2/C_3$ | $O_1/O_2$ | C/O |
| PCL ref/calc | 285.0 | 286.54 | 289.08 | 532.24 | 533.54 | 4 | 1 | 1 | 3 |
| PCL meas | 285.0 | 286.7 | 289.0 | 532.2 | 533.6 | 4.5 | 1.3 | 1.05 | 3.3 |
| PLLA ref/calc | 285.0 | 286.98 | 289.06 | 532.24 | 533.54 | 1 | 1 | 1 | 1.5 |
| P(LLA–CL) calc | | | | | | 1.9 | 1 | 1 | 1.95 |
| P(LLA–CL) meas | 285.0 | 287.1 | 289.2 | 532.2 | 533.7 | 3.0 | 1.2 | 1.2 | 2.8 |

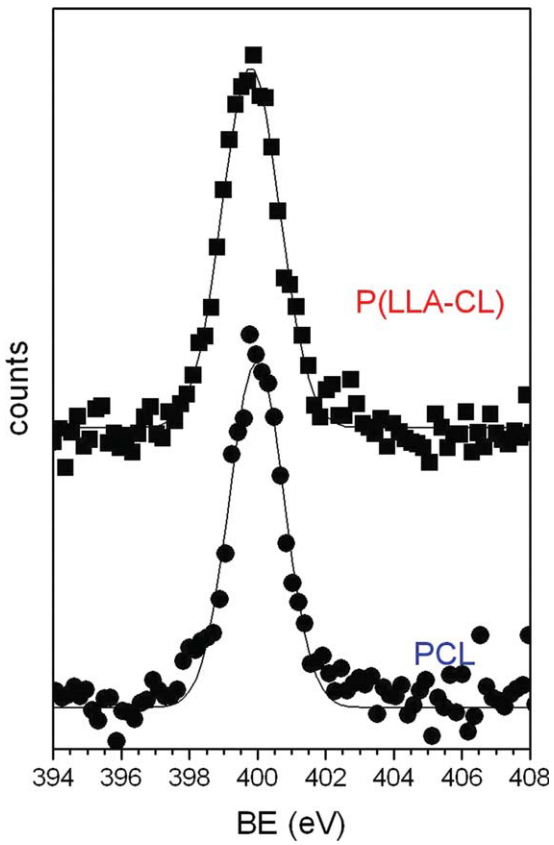


**Figure 5** N1s spectra of PCL and P(LLA–CL) mats after incubation with a 1.0 mg/mL RGD solution; markers represent experimental points, the line represents the fitting component. [Color figure can be viewed in the online issue, which is available at wileyonlinelibrary.com.]

both electrospun polymer scaffolds, although in a limited amount because the N/C and N/O measured, even for the samples prepared at a high peptide concentration, were less than 10% of the values calculated for the initial RGD peptide.

The carbon atoms of protein and peptides can be basically divided into three groups with different chemical environments: aliphatic C—C carbons of the amino acid pending groups (BE ≈ 285.0 eV), O=C—C—N carbons of the peptide backbone (BE = 286.5 eV), and highly antiscreened carbons of the peptide backbone (O=C—N, BE = 288.5) in increasing BE order.[33,34] Therefore, the curve-fitting analysis of the C1s and O1s spectra recorded after peptide immobilization was performed with the same component peaks used for the pristine polymer spectra. No relevant changes were detected in the spectra and in the related measured atomic ratios after peptide immobilization, as expected, because of the limited amount of peptide immobilized.

No changes were evidenced in the RAIRS spectra either; particularly, the amide I (in the range 1650–1620 $cm^{-1}$) and amide II (at about 1530 $cm^{-1}$) bands,[24,25] typical of peptides and proteins, could not be detected. This result was apparently in contradiction with the presence of peptide nitrogens detected by XPS. To account for this discrepancy, we had to remember that XPS and RAIRS have very different sampling depths: tenth of nanometers for XPS and micrometers for RAIRS. The results, therefore, confirmed the localization of the immobilized peptide on the outmost nanofiber surface.

RGD-conjugated scaffolds were evaluated for their capacity to enhance the adhesion (at 24 h) and proliferation (at 3 and 7 days) of human umbilical vein endothelial cells. These *in vitro* studies are the first step in the development of a small blood vessel substitute. Preliminary data showed that peptide

**TABLE IV**
**Measured N/C and N/O Ratios for the Polymer Nanofibers after Peptide Immobilization or Incorporation in the Melt and Comparison with the Calculated Values for the Corresponding Peptide**

| | | | Measured atomic ratios of the polymer nanofibers | | Calculated atomic ratios of the pristine peptide | |
|---|---|---|---|---|---|---|
| Polymer | Peptide | Concentration (mg/mL) | N/C | N/O | N/C | N/O |
| P(LLA–CL) | RGD | 1.0 | 0.022 | 0.057 | 0.36 | 1.11 |
| | | 0.10 | 0.009 | 0.019 | 0.36 | 1.11 |
| | | 0.010 | 0.006 | 0.014 | 0.36 | 1.11 |
| PCL | RGD | 1.0 | 0.023 | 0.1 | 0.36 | 1.11 |
| | | 0.10 | 0.008 | 0.033 | 0.36 | 1.11 |
| | | 0.010 | 0.005 | 0.02 | 0.36 | 1.11 |
| PCL | EAK | | 0.0154 | 0.045 | 0.31 | 0.875 |
| | DAK | | 0.0188 | 0.059 | 0.33 | 0.875 |
| | EAbuK | | 0.0166 | 0.048 | 0.276 | 0.875 |
| | EYK | | 0.0067 | 0.017 | 0.18 | 0.875 |
| | RGD–EAK | | 0.016 | 0.048 | 0.337 | 0.93 |
| | RGD–EAKsc | | 0.013 | 0.042 | 0.337 | 0.93 |

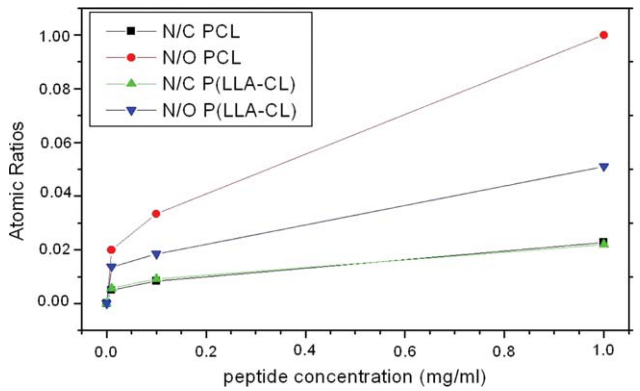


**Figure 6** Plot of the measured N/C and N/O atomic ratios for the PCL and P(LLA–CL) mats after incubation with the RGD solution as a function of the peptide concentration. [Color figure can be viewed in the online issue, which is available at wileyonlinelibrary.com.]

grafting to polymeric surface produced a significant enhancement in the cell adhesion up to 150% in the case of the PCL+RGD (1 mg/mL) scaffold with respect to the control. The proliferation of human umbilical vein endothelial cells was also positively influenced by the covalent functionalization with the RGD peptide, which showed a 20% increase for the PCL+RGD (1 mg/mL) scaffold and a 40% increase for the P(LLA–CL)+RGD (1 mg/mL) scaffold in comparison with electrospun polymeric scaffolds without peptide grafting.

### SA peptides

Polymeric nanofibers of PCL containing various SA peptides were also analyzed by XPS and RAIRS. For all of the investigated samples, XPS analysis evidenced an N1s signal at 400.0 eV related to peptide nitrogens (not shown): the measured atomic N/C and N/O ratios for the PCL nanofibers containing various SA peptides studied are shown in Table IV and compared with the values calculated for the respective SA peptides on the basis of the amino acid composition. The measured atomic ratios appeared to be in agreement with the values expected on the basis of the peptide/polymer weight ratio (5%). Only for EYK and RGD–EAKsc, the measured values were lower than expected. Relevant changes were also detected in the FTIR spectra. New small peaks appeared in the 1700–1500-$cm^{-1}$ region, which were related to amide I (C=O stretching) and amide II (N—H bending) vibrations of the peptide groups; both features can be seen in Figure 7, near the main C=O stretching band of the PCL ester function.

According to Haris and Chapman[24] and to Castano et al.,[25] the shape of the amide I band yields information on the peptide conformation. For α-helix and random-coil structures, the amide I band is found at about 1650 $cm^{-1}$, and for β sheets, it is found between 1620 and 1640 $cm^{-1}$. The lower the frequency is, the stronger the interchain hydrogen bond is. For a parallel β-sheet conformation, the amide I band is found at about 1635 $cm^{-1}$; for an antiparallel conformation, it is found at 1615–1625 $cm^{-1}$ because of stronger hydrogen bonds. The spectra of β-sheet peptides should also show a second amide I band at about 1680 $cm^{-1}$, which cannot be detected in our spectra because of the queue of the strong C=O stretching band of PCL.

To investigate the conformation of the peptide molecules in PCL nanofibers, a curve-fitting analysis of the FTIR spectra was performed, as shown in Figure 8. The C=O stretching of PCL was fitted with two component peaks at 1740 and 1720 $cm^{-1}$ plus a broad shoulder at 1690 $cm^{-1}$; the two peaks related to amide I stretching vibration were found at 1660 $cm^{-1}$ (α helix or random coil) and 1620 $cm^{-1}$ (β sheet), whereas the amide II band corresponded to the component at 1545 $cm^{-1}$. We tried to roughly estimate the percentage of peptides in the α-helix/random-coil or β-sheet conformation from the area ratio between the corresponding fitting components; the results are shown in Table V. The peptides EAK, EAbuK, DAK, and EYK appeared basically in β-sheet conformation; a higher percentage of α-helix/

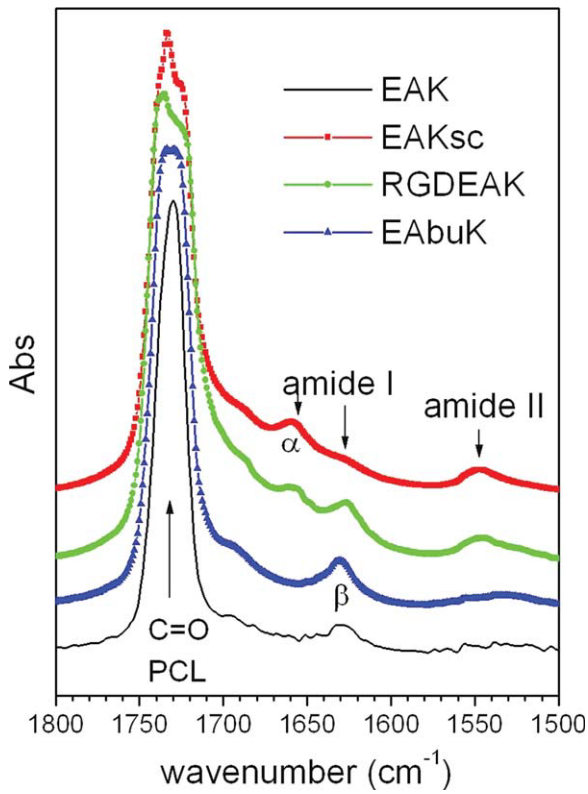


**Figure 7** FTIR spectra in the 1800–1500-$cm^{-1}$ range of PCL nanofibers containing different SA peptides. [Color figure can be viewed in the online issue, which is available at wileyonlinelibrary.com.]

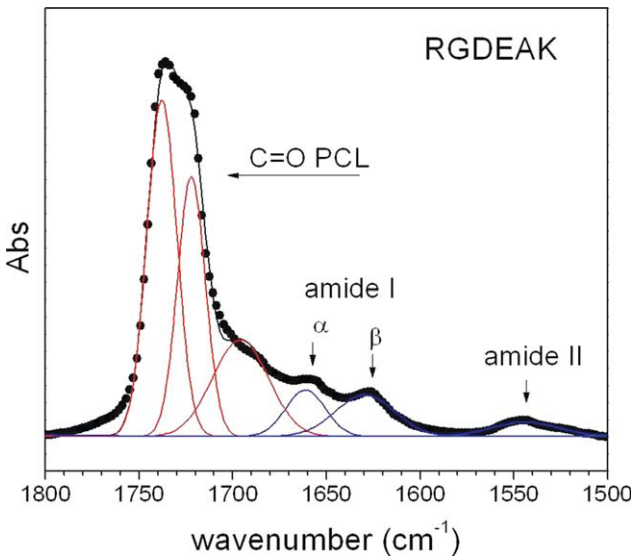


**Figure 8** Curve-fitting analysis of the FTIR spectrum in the 1800–1500-$cm^{-1}$ range of the PCL mat containing RGD–EAK peptide. The markers represent experimental points, and the lines represent fitting components and the calculated spectrum. [Color figure can be viewed in the online issue, which is available at wileyonlinelibrary.com.]

random-coil structure was evidenced for RGD–EAK, whereas RGD–EAKsc was predominantly an α helix/random coil. The conformation of SA peptide has been the object of previous FTIR studies;[10–12] the analysis of bulk samples and thick peptide films deposited on gold has evidenced a β-sheet conformation for all of the SA peptides, with the exception of RGD–EAKsc, that does not consist of a regular repetition of hydrophilic and hydrophobic amino acids and, therefore, has no SA capability. These results show that SA peptide incorporation into PCL nanofibers did not affect the peptide secondary structure, with only the exception of RGD–EAK, which showed a higher α-helix/random-coil percentage after incorporation into the PCL nanofibers than in the bulk system.

To investigate the stability of the unexpected RGD–EAK secondary structure, PCL/RGD–EAK nanofiber films were aged by incubation in saline buffered solution (see Experimental section); after aging, samples were investigated by FTIR spectroscopy and XPS. The SA process needed saline buffer treatment to arrange the peptide β sheet (present still in nonsaline solution) in a three-dimensional scaffold. In the FTIR spectra of the PCL/RGD–EAK nanofibers, changes after aging were evidenced in the amide I band; the curve-fitting analysis allowed us to calculate the new (α-helix/random-coil)/β-sheet percentages, also shown in Table V. The rearrangement of the peptide chains in the β-sheet conformation as a consequence of the aging process was evident.

The matrices produced by the addition of SA peptides to the PCL solution before electrospinning were used as scaffolds for *h*-osteoblasts. The *h*-osteoblast adhesion was higher for all of the scaffolds enriched with SA peptides in comparison with the PCL scaffold: the adhesion on the RGD–EAK scaffold was double with respect to the control (PCL). In particular, the scaffold enriched with EAbuK was able to significantly increase adhesion (at 4 h), the calcium deposition (at 7 days), and the expression of genes for osteopontin, alkaline phosphatase, and bone sialoprotein (at 24 h).

## CONCLUSIONS

Thin scaffolds of PCL and P(LLA–CL) nanofibers were successfully prepared by electrospinning.

The RGD adhesion peptide was immobilized on the nanofiber surface by incubation of polymer nanofibers with a photoreactive RGD–peptide and subsequent UV irradiation. The immobilized peptide remained confined on the nanofiber surface, and the amount of immobilized peptide increased with concentration in the mother solution, remaining very low even at the higher peptide concentration tested.

PCL/SA peptide nanofibers were also prepared by the incorporation of various SA peptides into the polymer solution. FTIR investigations showed that SA peptides incorporated into the PCL nanofibers retained their β-sheet conformation, with the exception of RGD–EAKsc, the non-SA peptide, and unexpectedly RGD–EAK, the peptide having the RGD adhesion motif coupled to the SA EAK sequence, that showed a considerable α-helix/random-coil percentage. Upon incubation with saline buffered solution, the α-helix/random-coil conformation percentage of RGD–EAK decreased considerably, and the peptide tended to rearrange in the SA-inducing β-sheet conformation.

**TABLE V**
**Percentage of α-Helix/Random-Coil and β-Sheet Peptide Conformations for SA Peptides in the PCL Nanofibers Measured from the FTIR Spectra**

| Aging | Peptide (%) | EAK | DAK | EAbuK | EYK | RGD–EAK | RGD–EAK aged | RGD–EAKsc |
|---|---|---|---|---|---|---|---|---|
| No. | β sheet | 89 | 85 | 90 | 88 | 57 | 75 | 30 |
| | α helix | 11 | 15 | 10 | 12 | 43 | 25 | 70 |

Preliminary biological assays performed on both kinds of peptide-containing polymer nanofibers yielded encouraging results.

The authors want to thank Paolo Pontini and Elena Bozza for their help in scaffold preparation.

## References


1. Spasova, M.; Malonova, N.; Paneva, D.; Mincheva, R.; Dubois, P.; Rashkov, I.; Maximova, V.; Danchev, D. Biomacromolecules 2010, 11, 151.
2. Paneva, D.; Bougard, F.; Malonova, N.; Dubois, P.; Rashkov, I. Eur Polym J 2008, 44, 566.
3. Luong-Van, E.; Grøndahl, L.; Ngiap Chua, K.; Leong, K. W.; Nurcombe, V.; Cool, S. M. Biomaterials 2006, 27, 2042.
4. Kim, H. I.; Matsuno, R.; Seo, J.-H.; Konno, T.; Takai, M.; Ishihara, K. Curr Appl Phys 2009, 9, e249.
5. Dettin, M.; Bagno, A.; Gambaretto, R.; Iucci, G.; Conconi, M. T.; Tucciotto, N.; Menti, A. M.; Grandi, C.; Di Bello, C.; Licciardello, A.; Polzonetti, G. J Biomed Mater Res A 2009, 90, 35.
6. Dettin, M.; Herath, T.; Gambaretto, R.; Iucci, G.; Battocchio, C.; Bagno, A.; Ghezzo, F.; Di Bello, C.; Polzonetti, G.; Di Silvio, L. J Biomed Mater Res A 2009, 91, 463.
7. Ma, P. X. Mater Today 2004, May, 30.
8. Holmes, T. C. Trends Biotechnol 2002, 20, 16.
9. Zhang, S.; Holmes, T. C.; Lockshin, C.; Rich, A. Proc Natl Acad Sci USA 2002, 90, 3334.
10. Polzonetti, G.; Battocchio, C.; Dettin, M.; Di Bello, C.; Iucci, G.; Carravetta, V. Mater Sci Eng C 2006, 26, 929.
11. Iucci, G.; Battocchio, C.; Dettin, M.; Gambaretto, R.; Polzonetti, G. Surf Interface Anal 2008, 39, 210.
12. Battocchio, C.; Iucci, G.; Dettin, M.; Carravetta, V.; Monti, S.; Polzonetti, G. Mater Sci Eng C 2010, 169, 36.
13. Chen, M. L.; Dong, M. D.; Havelund, R.; Regina, V. R.; Meyer, R. L.; Besenbacher, F.; Kingshott, P. Chem Mater 2010, 22, 421.
14. Zhang, Y. Z.; Wang, X.; Feng, Y.; Li, J.; Lim, C. T.; Ramakrishna, S. Biomacromolecules 2006, 7, 1049.
15. Ignatova, M.; Malonova, N.; Markova, N.; Rashkov, I. Macromol Biosci 2009, 9, 102.
16. Toshkova, R.; Manolova, N.; Gardeva, E.; Ignatova, M.; Yossifova, L.; Rashkov, I.; Alexandrov, M. Int J Pharm 2010, 400, 221.
17. Ignatova, M.; Manolova, N.; Toshokova, R. A.; Rashkov, I.; Gardeva, E.; Yossifova, L.; Alexandrov, M. Biomacromolecules 2010, 11, 1633.
18. Stoilova, O.; Ignatova, M.; Manolova, N.; Godjevargova, T.; Mita, D. G.; Rashkov, I. Eur Polym J 2010, 46, 1966.
19. Yuan, J.; Shen, J.; Kang, I. K. Polym Int 2008, 57, 1188.
20. Hiep, N. T.; Lee, B. T. J Mater Sci: Mater Med 2010, 21, 1969.
21. Bajgai, M. P.; Kim, K.-W.; Parajuli, D. C.; Yoo, Kim, W. D.; Khil, M.-S.; Kim, H. Y. Polym Degrad Stab 2008, 93, 2172.
22. Li, S.-F.; Chen J.-P.; Wu, W.-T. J Mol Catal B 2007, 47, 117.
23. Zhu, S.; Peng, H.; Yu, X.; Zheng, X.; Cui, W.; Zhang, Z.; Li, X.; Wang, J.; Weng, J.; Jia, W.; Li, F. J Phys Chem B 2008, 112, 11209.
24. Haris, P. I.; Chapman, D. Biopolymers 1995, 37, 251.
25. Castano, S.; Desbat, B.; Laguerre, M.; Dufourcq, J. Biochim Biophys Acta 1999, 1416, 176.
26. Grant, G. A. Synthetic Peptides: A User's Guide; Freeman: New York, 1992.
27. Lee, K. H.; Kim, H. Y.; Khil, M. S.; Ra, Y. M.; Lee, D. R. Polymer 2003, 44, 1287.
28. Moulder, J. F.; Stickle, W. F.; Sobol, P. E.; Bomben, K. D. Handbook of X-Ray Photoelectron Spectroscopy; Physical Electronics: Eden Prairie, MN, 1995.
29. Chiono, V.; Vozzi, G.; D'Acunto, M.; Brinzi, S.; Domenica, C.; Vozzi, F.; Ahluwalia, A.; Barbani, N.; Giusti. P.; Ciardelli, N. Mater Sci Eng C 2009, 29, 2174.
30. Ding, S. D.; Wang, Y. Z.; Rudd, C. D. Polym Degrad Stab 2009, 94, 1515.
31. Thanki, P. N.; Dellacherie, E.; Six, J. L. Appl Surf Sci 2006, 253, 2758.
32. Beamson, G.; Briggs, D. High-Resolution XPS of Organic Polymers—The Scienta ESCA300 Database; Wiley: New York, 1992.
33. Lebugle, A.; Subirade, M.; Gueguen, J. Biochim Biophys Acta 1995, 1248, 107.
34. Deligianni, D. D.; Katsala, N.; Ladas, S.; Sotiropoulou, D.; Amebee, J.; Missirlis, Y. F. Biomaterials 2001, 22, 1241.